Study of spray structure from non-flash to flash boiling conditions with space-time tomography

Jianguo Du[a,1,*], Guangming Zang[b,1], Balaji Mohan[a,c], Ramzi Idoughi[b], Jaeheon Sim[c], Tiegang Fang[d], Peter Wonka[b], Wolfgang Heidrich[b], William L Roberts[a]

[a] *Clean Combustion Research Center, King Abdullah University of Science and Technology, Thuwal, Makkah Province, Saudi Arabia*
[b] *Visual Computing Center, King Abdullah University of Science and Technology, Thuwal, Makkah Province, Saudi Arabia*
[c] *Transport Technologies Division, R&DC, Saudi Aramco, Dhahran, Eastern Province, Saudi Arabia*
[d] *Department of Mechanical and Aerospace Engineering, North Carolina State University, Raleigh, NC 27695, United States*

Abstract

Flash boiling and plume interaction are common phenomena occurring in gasoline direct injection (GDI) spray at throttling and low load engine conditions. Combined with optical engines and low-pressure vessels, several optical techniques, such as backlight imaging, Mie-scattering, and laser sheet imaging have been employed to study the flash boiling morphology. However, in the 2D images resulting from these techniques (projection views or planar imaging), the 3D information is lost. Those methods are then incapable of providing satisfactory information, especially for the study of multi-plume interaction in flash boiling spray, since multi-plume interaction is not a 2D event. This paper reports the implementation of a 4D tomographic reconstruction method from multi-view diffused back illumination (DBI) images, used for the first time in spray characterization. This cost-effective and time-saving method with a simple experimental setup clarifies the 3D spray structure and fuel trajectory change from non-flashing conditions to flare flash conditions, and quantifies the 3D characteristics of individual plumes in non-flash conditions.

Keywords: Flash boiling; plume interaction; 4D tomography; space-time reconstruction; GDI spray

Supplemental material is available and contents are listed after the conclusions section

1. Introduction

Flash boiling is an inevitable phenomenon that occurs at throttling and low load conditions in typical gasoline direct injection (GDI) engines and newly-developed gasoline compression ignition (GCI) engines; it happens when liquid fuel experiences a fast depressurization process and reaches a superheated state. Spray morphology, penetration length, cone angle, and droplet size are all greatly affected by this phenomenon [1, 2]. Although it has the potential to achieve improved atomization [3, 4], under severe flashing conditions it can also lead to spray collapse [5, 6] and wall impingement. The occurrence of spray collapse dramatically changes the designed in-cylinder fuel distribution, and wall impingement will result in undesirable emissions. Thus, the study of plume interaction and spray collapse process under flash boiling conditions is of preeminent concern.

Plume radial expansion and adjacent plume interaction under flash boiling conditions have been widely observed in experimental studies [7, 8]. Various techniques have been reported to characterize these behaviors. Diffused back illumination [9], Schlieren or shadowgraph [7, 10], and Mie scattering [11] techniques are commonly used for volume illumination, so that 2D projection views (integrated views) can then be captured. These techniques have the advantage of covering the entire spray field, but they cannot resolve the spray spatially along the line-of sight direction. Some techniques like diffused back illumination (DBI) have the problem of line of sight plume overlapping for multi-hole injectors, as shown in Figure 1 (e, f). Planar illumination (Mie-scattering [12] and fluorescence [13]) is another widely-used method to characterize the spray, but it only captures a cross-section layer of the spray. This method could decrease the interference of light signals from the out-of-plane zone to a certain extent,

[*]Corresponding author: jianguo.du@kaust.edu.sa
[1]These authors contributed equally to this work.

and it has the ability to resolve the inner structure of the spray, but this planar imaging method will intrinsically lose out-of-plane information. The spray collapse phenomenon in multi-hole GDI spray – rather than an in-plane behavior– is a result of a complex interaction among the multi-plumes circumferentially and radially. Thus, for a better understanding of the spray collapse phenomenon, resolving the 3D spray structure is of great importance. Moreover, individual plume cone angle and plume direction can easily be determined from the retrieved 3D structure, benefiting both regular GDI spray and diesel spray characterizations.

Spray structure reconstruction is not new in the field of spray characterization. 2D reconstruction was reported by Cho *et al.* [14], where a 514 nm laser beam was used to sweep a spray cross-section and measure the transmission rate. With a spray rotated at 18 angles, the spray cross-section shape was reconstructed using maximum likelihood estimation. Parrish *et al.* [15] implemented a planar line-of-sight laser extinction measurement for 2D tomography in a flash boiling spray. Eight view angles were obtained, and the maximum likelihood deconvolution scheme was used in the reconstruction framework. A 2D cross-section spray structure was given by this method. The same methods were later implemented by Sivathanu *et al.* [16] to determine the GDI spray plume centroid location. Sechenyh *et al.* [17] proposed a 3D reconstruction based on the assumption of a circular object cross-section, so that single-view X-ray or DBI (LED as a light source) 2D images could be used for the 3D reconstruction of dribble volume after the end of the injection. Kristensson *et al.* [18] used structured laser light illumination for extinction coefficient measurements. They captured 36 projection views to reconstruct a cold 3D GDI spray, by applying the filtered back projection (FBP) algorithm.

Various types of light sources (LED, laser, and X-ray) have been applied to 2D or 3D spray structure reconstruction. The X-ray is an excellent option to avoid multiple Mie-scattering signals in dense spray regions, but the high cost of instrumentation limits its wide application. Structured laser illumination is another option to suppress multiple Mie-scattering, but it has a relatively complex optical alignment. Even if its cost is less than the X-ray, it remains relatively more expensive than diffused back illumination (DBI). Its simple optical setup and low cost (LED can be used as a light source) make DBI a widely used method for liquid phase spray characterization.

As previously mentioned, the FBP algorithm was implemented for the tomographic reconstruction of the 3D structure of spray. This type of transform-based method relies on Radon transform and its inverse [19]. It offers fast reconstruction but it requires a large number of projections during the data capture process to achieve acceptable reconstruction results. In contrast, iterative tomographic reconstruction methods have been shown to yield better reconstruction results than transform-based methods for a small number of projections [20–22]. These methods are more suitable to the set up in this paper. Recently, a new 4D tomographic reconstruction method entitled *Space-time tomography* (ST-Tomography), based on iterative methods, was introduced by Zang *et al.* [23]. This approach simultaneously reconstructs a set of 3D volumes representing the scanned object or phenomenon at different time frames, and the motion fields between these volumes. By jointly recovering the 3D volumes and the motion fields, ST-Tomography transfers information across the entire time sequence. This strategy overcomes quality and resolution issues that occur when the 3D volumes are reconstructed independently. Details about the accuracy and reconstruction quality of ST-tomography method can be found in Zang et al. [23][24], in which different reconstruction methods have been compared and real x-ray scans of different types of objects have been tested.

To date, 3D reconstruction has not been directed to the study of plume interaction and spray collapse phenomenon. A LED-based cost-effective DBI method has been combined with an advanced 4D tomography algorithm to fill the gap in this study. This new method is evaluated here for its ability to resolve collapsed spray structure and determine the 3D direction of individual plumes. The results on flash boiling regarding the structure of collapsed spray are relevant to IC engines operating at throttling and low load conditions. Thus it helps reveal the in-cylinder fuel distribution and trajectory change, which will affect the later combustion and emission behavior[25].

2. Experimental setup and conditions

To simulate throttling and low load GDI engine spray conditions, relatively low ambient gas densities were tested in this work. As a result, spray penetration length was expected to be longer at these conditions. A large volume chamber (27 L) was used for the spray study (Figure 1 a), to avoid spray-wall interaction. A ten-hole gasoline injector was horizontally mounted in the chamber with the ability to rotate around the injector axis. The fixture for the injector (Figure 1 b) had an internal channel for thermal bath fluid, set to maintain the fuel temperature at 90 °C. Figure 1(c) and (d) show the nozzle holes and plumes distribution at an initial position (reference position).

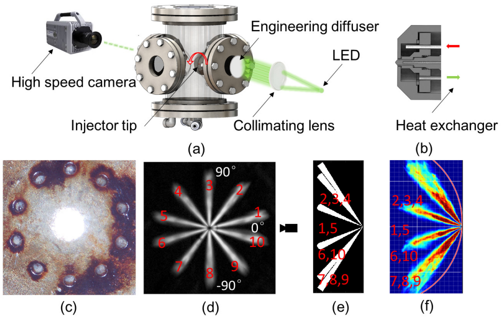

Figure 1: (a) Optical alignment; (b) injector fixture with built-in thermal bath channel; (c) injector nozzle hole orientation; (d) Mie-scattering from front of spray;(e,f) sketch and DBI image showing the overlap of plumes along the line of sight, respectively

The optical alignment is shown in Figure 1(a). A pulsed-driven white LED was used as the light source. A Photron SA-X2 high-speed camera was employed at 40 kfps with a resolution of 552×512 pixels (0.1425 mm/pixel) to capture the extinction images. For 2D or 3D reconstruction, the injector was usually rotated for different views. Injector rotation was performed mainly because of the optical access limitations for simultaneous multi-view and large view number requirements by the reconstruction algorithms; injector rotation also offers consistent spray morphology under fixed conditions. In this work, the injector was rotated at a step of ten degrees for 180 degrees, covering 19 view angles in total. At each view angle, the averaged image of three repeats was used for 3D reconstruction. Figure 2 shows a comparison of the averaged image and the corresponding three repeats in three representative conditions (collapsing, transitional, and non-flashing). R_p is the ratio of ambient gas pressure to saturation vapor pressure. Individual images can show the sharp small-scale structures that become smudged in the averaged image. However, these small-scale structures are not necessarily the same for all spray events that are rotated at different view angles. The averaged image was more representative since it maintained the large-scale structure and fuel distribution, so averaged images were used for reconstruction.

Details of the experimental conditions are listed in Table 1. Ambient gas pressure (P_a) was varied so that, R_p (the ratio of P_a to saturation vapor pressure P_s (77.42 kPa at 90 °C [26])) covered the range from 0.05 to 1.4, and with refinement in the flash boiling regime. The definition of different regimes for this injector can be referenced from previous work by this group[27].

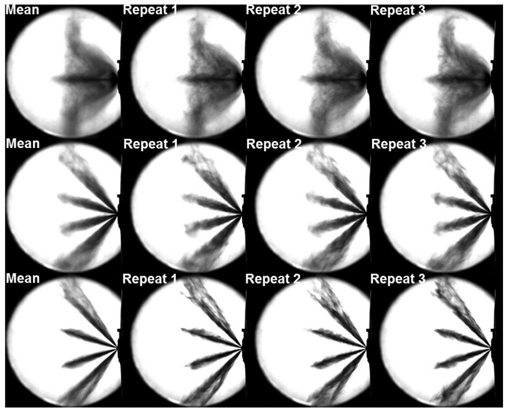

Figure 2: Comparison of averaged image and corresponding three repeats, from top to bottom: R_p = 0.05, 0.5, 1.4, view angle = 0°, Time after start of injection (aSOI) = 0.725 ms

Table 1: Experimental conditions

Ambient gas			N_2				Injection pressure				100 bar			
Injection duration			1 ms				Designed cone angle				110 °			
Orifice diameter			165 μm				Fuel				*iso*-octane			
T_{fuel}			90 °C				T_{amb}				23 °C			
$P_{amb}(kPa)$														
4	8	12	15	19	23	31	39	46	54	62	69	77	92	108
$R_p = P_a/P_s$														
0.05	0.1	0.15	0.2	0.25	0.3	0.4	0.5	0.6	0.7	0.8	0.9	1	1.2	1.4

3. 4D reconstruction algorithm

3.1. Formulation and solver

The ST-Tomography [23] is utilized to reconstruct the spray structure for all experiments discussed in this paper. This 4D tomography framework is based on a variational approach that jointly estimates the density volume field (the 3D spray structure) and the deformation vector field. In this method, the spray reconstruction is formulated as an optimization problem shown in the following equation:

$$
\begin{aligned}
(\mathbf{f}^*, \mathbf{u}^*) = \;& \underset{\mathbf{f},\mathbf{u}}{\operatorname{argmin}} \sum_{t=1}^{N_t} \|\mathbf{A}\mathbf{f}_t - \mathbf{p}_t\|_2^2 \\
&+ \kappa_1 \sum_{t=1}^{N_t} \|\nabla_S \mathbf{f}_t\|_{\mathrm{H}_\epsilon} + \kappa_2 \sum_{t=1}^{N_t-1} \sum_{i=x,y,z} \left\|\nabla_S \mathbf{u}_{t,i}\right\|_{\mathrm{H}_\tau} \\
&+ \kappa_3 \sum_{t=1}^{N_t} \|\nabla_T \mathbf{f}_t\|_2^2 + \kappa_4 \sum_{t=1}^{N_t-1} \|\nabla_T \mathbf{f}_t + \nabla_S \mathbf{f}_t \cdot \mathbf{u}_t\|_1
\end{aligned}
\tag{1}
$$

Where, $\mathbf{f} = (\mathbf{f}_t)_{t=1...N_t}$ and $\mathbf{u} = (\mathbf{u}_t)_{t=1...N_t}$ respectively represent the spray density field and the deformation field for the N_t time steps. The operators ∇_S and ∇_T correspond to the spatial and temporal discrete gradient. $\mathbf{p}_t$ are the projection views (measurements) captured at time step t, and $\mathbf{A}$ is the matrix that models the Radon transform operator for the captured projection views. κ_1, κ_2, κ_3, and κ_4 are relative weights for the different priors used in this optimization. The first term of the minimization problem is the data fidelity term, which ensures a good fit for the reconstructed spray density with the measurement videos. The second and third terms are spatial priors applied on the spray density field and the deformation field, respectively, to ensure smooth spatial results. The last two priors act as temporal priors to ensure consistent results in the time domain. The fourth one is a temporal smoothness of the spray density field, while the last one can be interpreted as a temporal coherence prior that involves both the spray density and the deformation field.

This optimization problem is then subdivided into two sub-problems: the spray structure reconstruction and the deformation field estimation. These two subproblems are solved alternatively in an iterative manner, by using the first-order primal-dual framework introduced by Chambolle and Pock [28]. Moreover, the proximal Simultaneous Algebraic Reconstruction Technique (PSART algorithm), developed in [21], is used to solve the tomography problem included in the data fidelity term in Equation 1.

3.2. Parameters setting

For the purpose of reconstruction, some parameters are required, or have to be tuned. The spray structures were captured from 19 projection views uniformly distributed over 180 degrees. The distance between the optical camera and the iso-center of the spray is 800 *mm*, while the distance between the optical camera and the diffuser is 1050 *mm*. These two distances are required, as well as the projections angles, for the calculation of the matrix **A** (see Equation 1). As previously described, the experiment was conducted for 15 different conditions; for each condition, a video sequence of 60 images (time steps) was captured with the high speed camera. After a pre-processing step, the $\mathbf{p}_t$ projection views were obtained from the raw captured images. The size of each projection image was 552×512, with a pixel size of 0.142 *mm*. The reconstructed volume size at each time step was 150×130×150, with a voxel size 0.5 *mm*. Finally, for all experiments conducted, the weights of the optimization priors were set as follows: $\kappa_1 = 0.15$, $\kappa_2 = 0.2$, $\kappa_3 = 0.5$ and $\kappa_4 = 0.1$. All parameters were identical in reconstructing different conditions. Reconstruction was conducted on a computer with 512 GB RAM and a dual-core 3.00GHZ Intel Xeon processor. The framework is implemented in C++ and parallelized using OpenMP. At the current volume resolution setting, it takes around 55 seconds and 38 Mb physical storage space to reconstruct the volume for each time frame.

Number of projection views is also an important parameter, which affects the experimental practicability, reconstruction quality, as well as computational cost. A parametric study of view number's influence is operated and the results are shown in Figure 3. Reconstructions are conducted based on 4, 7, 10, and 19 of uniformly distributed view angles covering 180° (at a step of 60°, 30°, 20°, 10° respectively). With the decrease of view numbers, the reconstruction quality degrades. It should be noted that in this work the averaged image of three repeats at each view angle was used for reconstruction. Using multiple cameras to simultaneously capture the spray from different view angles will definitely improve the reconstruction quality, but this is experimentally not affordable limited by the optical access of setups like constant volume chamber and optical engines. However, this work demonstrated the possibility of 3D spray reconstruction for cases with limited optical access by rotating the injector. In the following sections, reconstruction results from 19 projection views are used for the discussions.

4. Results and discussions

4.1. 3D spray structure

Figure 4 shows the 3D view of sprays at different ambient gas pressures (0.125 ms, 0.375 ms, and 0.625 ms aSOI). From 77 kPa to 39 kPa, the spray had ten separated plumes (up most and down most plumes are plume 3 and 8 respectively, which is consistent with the definition in Figure 1 d), while at 23 kPa, some plumes(5-6, 10-1) became connected by interaction. At 12 kPa, a bowl-shaped closed spray cone was formed by plume interactions. The original plume direction was diluted and became transparent. At 4 kPa, droplets were concentrated onto the central plane between adjacent plumes. The central dark area, shown in Figure 2 (4 kPa case), was caused by circumferential collapsing between plumes 5~6 and 10~1 (defined in Figure 7). Besides, plumes collapse radially towards the injector axis. In the center area of the spray cone, four concentrated main branches (formed by plume interaction 9-10-1-2, 2-3-4, 4-5-6-7, and 7-8-9, defined in Figure 7) were connected and developed along the injector axis. This phenomenon was confirmed by laser sheet imaging and reconstructed volume slice shown in Figure 5.

4.2. Reconstruction validation

Planar laser light imaging was also performed to validate the 3D reconstruction technique. At 10 and

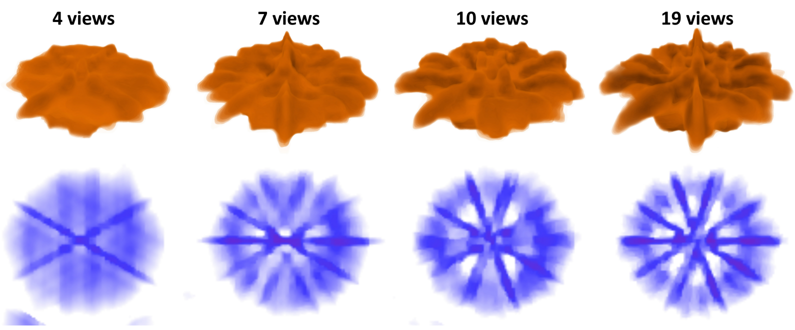

Figure 3: Parametric study of view number's effect on reconstruction quality: top row shows the reconstructed volume; bottom row shows the slice at 20 mm downstream of injector nozzle

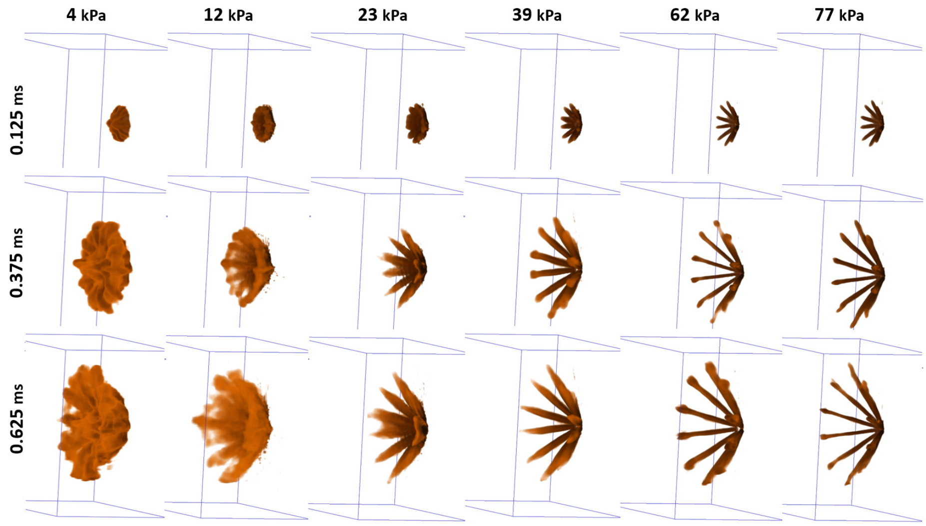

Figure 4: 3D reconstruction results of spray at various instants of time. (Videos are included in supplemental materials)

15 mm downstream of the injector tip, scanning was performed for six representative cases, covering the collapsing regime, transitional regime, and the non-flashing regime. Each condition was repeated 20 times, and the averaged cross-section images were used for comparison. Due to the multiple scattering effects, scattered light from an object close to but outside the laser plane was also captured by the camera, especially at the dense spray regions. Thus, the results of the laser sheet imaging were not a perfect slice of spray volume. Furthermore, the extinction of laser intensity along the line of sight could result in an image with non-uniform brightness, small droplets, or a diluted region might not be illuminated well by the attenuated laser. Laser sheet energy profile is also important for image quality. As shown in Figure 5 and Figure 6, a brighter top area and a darker bottom area occurred because of this artificial non-uniformity of energy profile. Because of these shortcomings in the laser sheet imaging, it cannot be considered ground truth; therefore only qualitative rather than quantitative comparisons were possible.

Figure 5 shows the comparison between laser sheet imaging and reconstructed volume slice at a wide scanning range(5 to 30 mm from the injector tip) for the 4 kPa case. Note that the geometric scales of all sub-images from both methods are identical, and the intensity of each sub-image is normalized. With increasing distance from the injector tip, the cross-section dimension and pattern obtained from reconstructions agreed well with the laser imaging results, except at the near nozzle region (5 mm from injector tip). In this region, the central area of spray in the laser sheet imaging was bright due to strong multiple scattering at the spray dense region. However, from the reconstructed slice, a relatively hollow central region can be seen, indicating that the spray collapsed to the injector axis

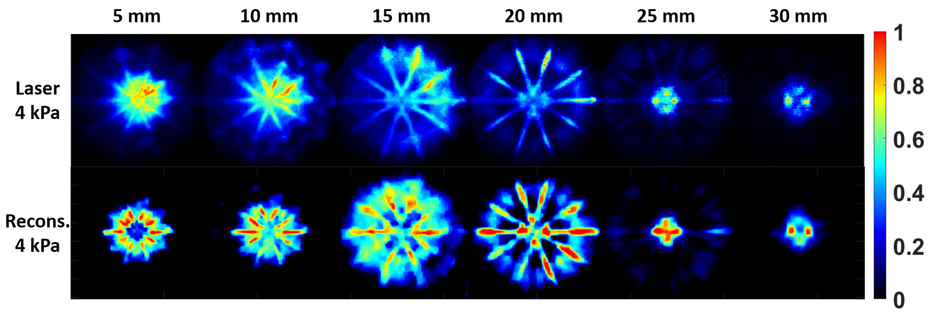

Figure 5: Laser sheet images and reconstructed volume slices at different heights from injector tip (4 kPa ambient gas pressure, time aSOI = 0.4 ms).

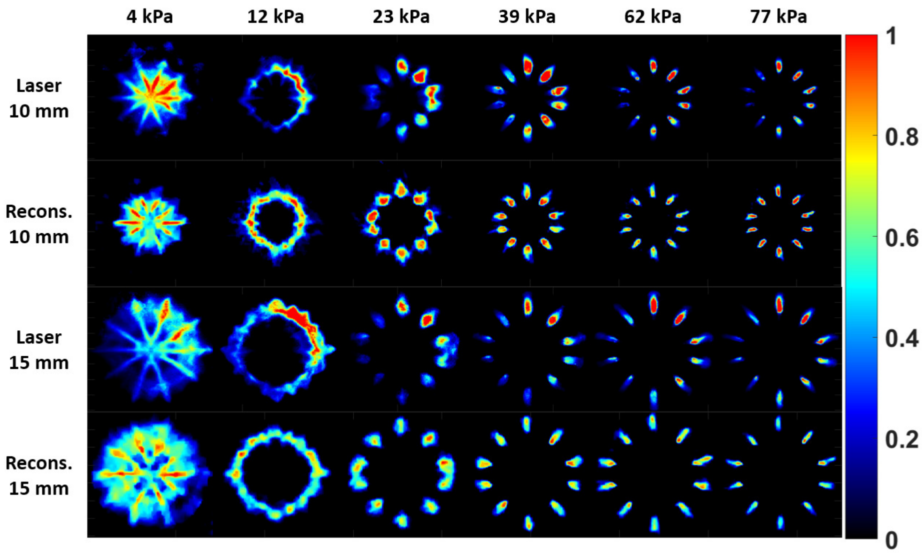

Figure 6: Experimental validation for reconstruction quality with laser sheet imaging. Reconstructed volume at $time\ aSOI = 0.4\ ms$ is selected. From left to right: Different ambient gas pressures. From top to bottom: Different slice locations (physical distances to injector at 10 and 15 mm) are presented, respectively.

after a certain distance downstream from the injector tip. This reconstructed results agree with the projection view shown in Figure 2. Figure 6 shows the comparison of the two methods for six representative cases. From the non-flash condition to the collapsing regime, the reconstructed results showed a very consistent cross-section spray pattern and size with laser imaging. From 77 kPa to 39 kPa, plume swelling was captured by both methods. When the ambient gas pressure decreased to 23 kPa, adjacent plume interaction first began at the two horizontal plume pairs (plumes 5~6 and 10~1 in Figure 7). This feature was also successfully resolved by reconstruction. At 12 kPa, interaction occurred between all the adjacent plumes, and a closed circle shaped cross-section formed. When ambient gas pressure decreased further, the spray cone was no longer hollow at the scanned locations, meaning that the plumes collapsed towards the injector axis and a central jet formed. Moreover, aggregation of droplets shifted from the direction of the originally designed plume to the central plane between two adjacent plumes. These aggregation features and the cavity on the original plume direction in the central part were both successfully captured by the reconstruction. The above comparison demonstrated that the 4D reconstruction algorithm successfully resolved spray structure and can visually aid in understanding spray structure at flash boiling conditions.

4.3. 3D direction of plumes

In addition to clarifying the inner structure of the collapsed spray, the 4D tomographic reconstruction also makes it possible to quantify the direction, cone angle, and penetration length of each individual plume. This advantage can potentially benefit spray simulations by giving the initial and boundary conditions of each plume, rather than assuming symmetrical plumes, which is invalid due to manufacturing capabilities. To collect this information experimentally, it usually requires a combination of laser sheet imaging from various views (parallel and perpendicular to the injector axis), which mandates changes to the setup as well. Moreover, the alignment of the laser sheet with each plume is not as simple as the method introduced in this work. Because it requires iterative adjustment of injector orientation and taking image of spray to make sure laser sheet goes through plume's center line.

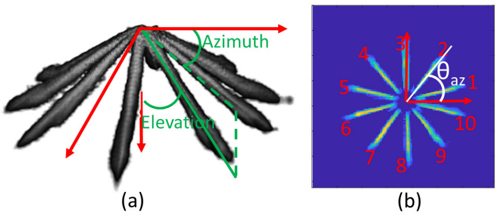

Figure 7: Definition of plume numbering and 3D direction

Figure 7 (a) shows the definition of 3D plume direction. From the projection view (b) of 3D volume, the azimuthal angle of each plume is defined as θ_{az} (from 0° to 360°). The angle between two adjacent plumes can be further determined ($\theta_{az,i\sim i+1}$). With the slice on these directions, the elevation angle of each plume can be measured. Table 2 shows the direction of each plume measured at 108 kPa and time aSOI = $0.4ms$. Individual plume angle is consistent with the cone angle designed by the manufacture (55°). The angle between two adjacent plumes (plumes 5~6 and 10~1) shows a smaller value than the other pairs, confirmed by the projection view shown in Figure 7(b). Due to this asymmetrical behavior, it would be incorrect to assume symmetrical plume directions in CFD for GDI injectors, since plume directions are a vital parameter in CFD modeling of GDI injectors [29, 30].

Table 2: Plume 3D direction (P_{amb}= 108 kPa, Time aSOI = 0.4 ms)

Plume	1	2	3	4	5	6	7	8	9	10
$\theta_{az}(°)$	14	51	92	133	168	196	233	271	308	346
$\theta_{az,i\sim i+1}(°)$	37	41	41	35	28	37	38	37	38	28
$\theta_{el}(°)$	54	52	56	53	55	54	55	57	54	53

5. Conclusions

A new method was proposed for spray characterization, based on DBI and space-time tomography. Qualitative validation with laser sheet imaging proves the ability of 4D tomography to resolve a 3D spray structure. This method can help examine spray collapse phenomena occurring at high pressure conditions, normal in high load GDI engines[31], or GCI engines. In addition, 4D tomography can be implemented for other purposes, such as dribble volume measurements in fuel sprays. Further, the 4D tomography can also be extended for soot 3D distribution measurement combined with DBI extinction imaging[32].

With the help of 3D visualization, plume interaction and collapsed spray structure were revealed. At the transitional regime, the interaction first began at adjacent plumes with the smallest angle (or gap) between them. When superheat intensity increased further, the adjacent plume interaction occurred to all plumes, and a closed bowl-shaped spray cone formed. These were the circumferential spray collapse. At the same time, a radial collapse coexisted, causing a decrease in the spray cone angle. Under extreme flare flash conditions, the liquid fuel aggregated onto the central plane between two adjacent plumes. The ten layers formed by the collapse of ten plumes were connected at the injector axis, shown as a central jet.

The reconstructed 3D spray also made it possible to determine the direction of individual plumes, these directions helped understand the plume interactions and spray collapse phenomenon. The shown asymmetry of plumes offered guidance for CFD analysis that the assumption of symmetrical plumes is not recommended for GDI injectors, making the measurement of individual plume direction desirable. In addition, qualitative comparison of collapsed spray structure and quantitative comparison of real individual plume length can be provided for CFD modeling validation. The cost saving and easy setup method introduced in this work has great potential to be popularized for this purpose.

List of Supplemental Material

- Video S1: A comparison of reconstructed 3D spray under various ambient gas pressures

Acknowledgements

This work was sponsored by Saudi Aramco under the FUELCOM II program, CCRC and VCC Center Competitive Funding, and Competitive Research Grants from KAUST.

References

[1] B. Bhatia, A. De, Flash boiling in sprays: Recent developments and modeling, Journal of the Indian Institute of Science (2019).

[2] Z. Wang, B. Wang, C. Jiang, H. Xu, T. Badawy, Microscopic characterization of isooctane spray in the near field under flash boiling condition, Applied energy 180 (2016) 598–606.

[3] C. Jiang, M. C. Parker, J. Helie, A. Spencer, C. P. Garner, G. Wigley, Impact of gasoline direct injection fuel injector hole geometry on spray characteristics under flash boiling and ambient conditions, Fuel 241 (2019) 71–82.

[4] H. Guo, X. Ma, Y. Li, S. Liang, Z. Wang, H. Xu, J. Wang, Effect of flash boiling on microscopic and macroscopic spray characteristics in optical gdi engine, Fuel 190 (2017) 79–89.

[5] M. Xu, Y. Zhang, W. Zeng, G. Zhang, M. Zhang, Flash Boiling: Easy and Better Way to Generate Ideal Sprays than the High Injection Pressure, Technical Report 1, 2013.

[6] L. Wang, F. Wang, T. Fang, Flash boiling hollow cone spray from a gdi injector under different conditions, International Journal of Multiphase Flow 118 (2019) 50–63.

[7] J. Lacey, F. Poursadegh, M. J. Brear, R. Gordon, P. Petersen, C. Lakey, B. Butcher, S. Ryan, Generalizing the behavior of flash-boiling, plume interaction and spray collapse for multi-hole, direct injection, Fuel 200 (2017) 345–356.

[8] P. Aleiferis, Z. van Romunde, An analysis of spray development with iso-octane, n-pentane, gasoline, ethanol and n-butanol from a multi-hole injector under hot fuel conditions, Fuel 105 (2013) 143–168.

[9] S. Wu, S. Yang, M. Wooldridge, M. Xu, Experimental study of the spray collapse process of multi-hole gasoline fuel injection at flash boiling conditions, Fuel 242 (2019) 109–123.

[10] Y. Huang, S. Huang, R. Huang, G. Hong, Spray and evaporation characteristics of ethanol and gasoline direct injection in non-evaporating, transition and flash-boiling conditions, Energy conversion and management 108 (2016) 68–77.

[11] A. Montanaro, L. Allocca, Flash boiling evidences of a multi-hole GDI spray under engine conditions by Mie-scattering measurements, Technical Report, 2015.

[12] W. Zeng, M. Xu, G. Zhang, Y. Zhang, D. J. Cleary, Atomization and vaporization for flash-boiling multi-hole sprays with alcohol fuels, Fuel 95 (2012) 287–297.

[13] G. Zhang, M. Xu, Y. Zhang, W. Zeng, Quantitative Measurements of Liquid and Vapor Distributions in Flash Boiling Fuel Sprays using Planar Laser Induced Exciplex Technique, 2011.

[14] S. Cho, G. Park, Y. Yoon, Dense spray patternation using optical tomography, International Journal of Aeronautical and Space Sciences 14 (2013) 398–407.

[15] S. Parrish, R. Zink, Y. Sivathanu, J. Lim, in: ILASS-Americas 22nd annual conference on liquid atomization and spray systems, Cincinnati, OH.

[16] Y. Sivathanu, J. Lim, V. Kulkarni, Time-dependent line-of-sight extinction tomography for multi-hole gdi injectors, International Journal of Spray and Combustion Dynamics 9 (2017) 199–211.

[17] V. Sechenyh, D. J. Duke, A. B. Swantek, K. E. Matusik, A. L. Kastengren, C. F. Powell, A. Viera, R. Payri, C. Crua, Quantitative analysis of dribble volumes and rates using three-dimensional reconstruction of x-ray and diffused back-illumination images of diesel sprays, International Journal of Engine Research (2019) 1468087419860955.

[18] E. Kristensson, E. Berrocal, M. Aldén, Quantitative 3d imaging of scattering media using structured illumination and computed tomography, Optics Express 20 (2012) 14437–14450.

[19] L. A. Feldkamp, L. Davis, J. W. Kress, Practical cone-beam algorithm, Josa a 1 (1984) 612–619.

[20] A. H. Andersen, Algebraic reconstruction in ct from limited views, IEEE transactions on medical imaging 8 (1989) 50–55.

[21] G. Zang, M. Aly, R. Idoughi, P. Wonka, W. Heidrich, in: Proceedings of the European Conference on Computer Vision (ECCV), pp. 137–153.

[22] X. Pan, E. Y. Sidky, M. Vannier, Why do commercial ct scanners still employ traditional, filtered back-projection for image reconstruction?, Inverse problems 25 (2009) 123009.

[23] G. Zang, R. Idoughi, R. Tao, G. Lubineau, P. Wonka, W. Heidrich, Space-time tomography for continuously deforming objects, ACM Transactions on Graphics (TOG) 37 (2018) 100.

[24] G. Zang, R. Idoughi, R. Tao, G. Lubineau, P. Wonka, W. Heidrich, Warp-and-project tomography for rapidly deforming objects, ACM Transactions on Graphics (TOG) 38 (2019).

[25] R. Kale, R. Banerjee, Spray Collapse in a Multi-hole GDI Injector and Its Effect on In-Cylinder Combustion, Springer Singapore, Singapore, pp. 43–61.

[26] C. B. Willingham, W. J. Taylor, J. M. Pignocco, F. D. Rossini, Vapor pressures and boiling points of some paraffin, alkylcyclopentane, alkylcyclohexane, and alkylbenzene hydrocarbons, Journal of Research of the National Bureau of Standards 35 (1945) 219–244.

[27] J. Du, B. Mohan, J. Sim, T. Fang, W. L. Roberts, Study of spray collapse phenomenon at flash boiling conditions using simultaneous front and side view imaging, International Journal of Heat and Mass Transfer (2019) 118824.

[28] A. Chambolle, T. Pock, A first-order primal-dual algorithm for convex problems with applications to imaging, Journal of mathematical imaging and vision 40 (2011) 120–145.

[29] K. Saha, S. Som, M. Battistoni, Y. Li, S. Quan, P. Kelly Senecal, Modeling of internal and near-nozzle flow for a gasoline direct injection fuel injector, Journal of Energy Resources Technology 138 (2016).

[30] B. Mohan, M. Jaasim, F. H. Perez, J. Sim, W. Roberts, H. Im, in: Proceedings of the 10th International Symposium on Cavitation (CAV2018), ASME Press, 2018.

[31] P. Sphicas, L. M. Pickett, S. A. Skeen, J. H. Frank, Inter-plume aerodynamics for gasoline spray collapse, International Journal of Engine Research 19 (2018) 1048–1067.

[32] G. Zang, R. Idoughi, C. Wang, A. Bennett, J. Du, S. Skeen, W. Roberts, P. Wonka, W. Heidrich, in: Proceedings of the IEEE Conference on Computer Vision and Pattern Recognition (CVPR), IEEE, 2020.